Progress In Electromagnetics Research M, Vol. 99, 81–90, 2021

Liquid-Crystal Based, Beam-Steerable Quasi-Periodic Substrate Integrated Waveguide Leaky-Wave Antenna with Transverse Slots

Rodrigue B. Tchema and Anastasis C. Polycarpou*

Abstract—In this paper, a substrate integrated waveguide (SIW) quasi-uniform leaky-wave antenna (LWA) is proposed for a dynamically steerable beam design at a single frequency through the use of a thin layer of nematic liquid crystal (LC) underneath the substrate. The orientation of the LC molecules, and therefore the effective dielectric properties of the LC cell, is controlled via an externally low-frequency, low-strength bias voltage. The radiation occurs through a series of closely placed transverse slots etched on the top plane of the SIW. This antenna was designed to operate based on the fundamental space harmonic ($n = 0$) in the frequency range between 24.25 GHz and 29 GHz, which covers one of the future 5G frequency bands to be deployed in some parts of the world. This novel antenna design concept was verified numerically using a commercial software based on the Finite Element Method (FEM), and the results are presented and discussed herein.

1. INTRODUCTION

Leaky-wave Antennas (LWAs) use an electrically long guiding structure as the main mechanism of radiation. As the wave travels along the length of the structure, it leaks out energy (through radiation) into free space [1, 2]. The first leaky-wave antennas were based on rectangular conductive waveguides which were bulky, heavy, costly, and difficult to fabricate. Substrate integrated waveguides (SIWs) [3, 4] have specific advantages over traditional waveguides allowing their use in planar microwave and millimeter-wave applications [5]. Specifically, SIWs are characterized by low-cost production, ease of fabrication, low energy dissipation, light-weight structure, and ease of integration with planar circuits and electronic boards [6].

One of the main properties of LWAs is their beam-scanning capability. Scanning of the main beam is achieved through variation of the operating frequency of the antenna. In many occasions, however, it is important that the space is scanned at a fixed frequency. For this particular scenario, a conventional LWA design will not be applicable. This is a major drawback of the traditional LWA designs as there is no effective tuning mechanism for continuous beam scanning at a single frequency.

In the past two decades, liquid crystals (LCs) [7, 8] — due to their electro-optic properties — have appeared as a promising solution to the aforementioned limitation of this type of antenna. By imposing a low-frequency, low-strength, external electric field across the LC cell, the molecules of the LC compound orient themselves according to the strength of the bias voltage. This causes the effective complex permittivity of the material to change accordingly, thus tuning propagation characteristics of the supported waveguide mode. It is also important to emphasize that new generation of LC compounds have inherently low losses, improved tuning capabilities based on birefringence, and relatively low-power consumption. These properties of LCs allow for their use in the design of millimeter and microwave tuning devices.

Received 14 September 2020, Accepted 24 November 2020, Scheduled 1 December 2020
* Corresponding author: Anastasis C. Polycarpou (polycarpou.a@unic.ac.cy).
The authors are with the Department of Engineering, University of Nicosia, Cyprus.

Examples of tunable devices include delay lines [9, 10], phase shifters [11, 12], tunable filters [13, 14], and frequency-agile microstrip antennas [15–19]. It has been shown in [20] that a tunable band-pass filter based on SIW and LC technology could also be achieved with magnetic biasing using external electromagnets, which are often heavy and bulky. In [21], it has been demonstrated that biasing of a SIW-based filter using an external electric field could be achieved by loading rectangular patches in SIW cavity. A half-mode SIW-LWA was designed in [22] illustrating a 16-degrees main-beam deflection through tuning of the LC layer made by inserting a rectangular DC ground inside the waveguide.

Most of the research done on LC-based tunable antennas is related to microstrip patches. The applied bias voltage is used to tune the operating frequency of the antenna thus providing frequency agility. In this paper, we present a concept design where a thin layer of nematic LC is used underneath the substrate of a LWA based on SIW technology. The anisotropic properties of the LC compound were exploited in order to achieve scanning capability at a fixed operating frequency. This concept was recently presented in [23], where the ability to dynamically scan the main bean of the pattern through biasing of the LC was demonstrated for an SIW-LWA operating between 10 and 12.5 GHz (X-band). This paper is a continuation of this work showing an alternative design in mm-wave range, where the liquid crystal compounds are more suitable as their inherent losses tend to diminish. The proposed antenna design operates in the fundamental TE_{10} mode in the frequency range of 24.25–29 GHz. This particular concept design could be used as a low-power, small-cell (pico or fempto cells) antenna for future 5G wireless networks.

2. ANTENNA CONFIGURATION AND DESIGN

2.1. Antenna Geometry

The geometry of the proposed LWA based on SIW and LC technologies is depicted in Fig. 1. A Rogers RT/duroid 5870 (tm) substrate is used which has a relative permittivity of $\epsilon_r = 2.33$, a loss tangent $\tan\delta = 0.0012$, and a thickness $h = 0.254\,\text{mm}$. The corresponding width of the dielectric layer is $W = 16\,\text{mm}$. The total length of the antenna is $L = 156.5\,\text{mm}$ consisting of 3 main sections: The radiating section of length $L_r = 107\,\text{mm}$, another section with tapered slots on both sides of length $L_1 = 15\,\text{mm}$, and the microstrip lines of length $L_m = 9.75\,\text{mm}$.

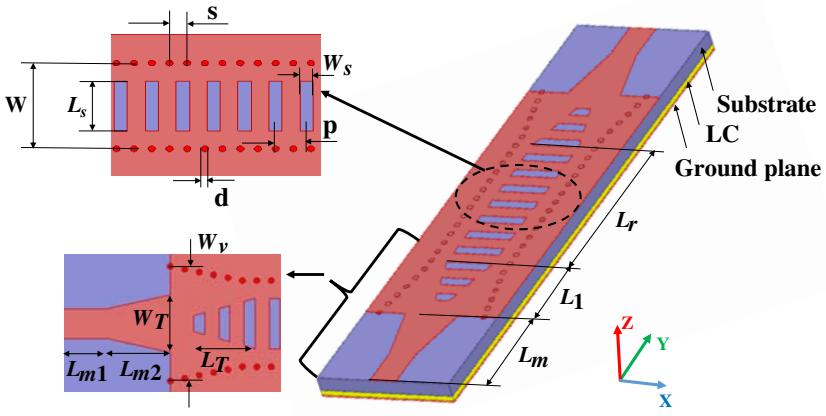

Figure 1. Geometry of the proposed LWA antenna based on SIW and LC technologies.

The period, i.e., the distance between adjacent slots, was chosen to be $p = 2.0\,\text{mm}$. A total of 69 slots were used as radiating elements along the length of the antenna. Each slot has a length of $L_s = 2.0\,\text{mm}$ and a width of $W_s = 0.35\,\text{mm}$. Since the period is small compared to the wavelength, the antenna radiates based on its fundamental ($n = 0$) space harmonic in the forward quadrant. The operating mode of this antenna is the TE_{10} and the slots are tapered at both ends over a distance $L_T = 10\,\text{mm}$ in order to reduce reflection loss. The length of the slots was gradually reduced from 2.0 mm to 0.02 mm, while the slot width was maintained unchanged. A tapered microstrip line of length

$L_m = 9.75\,\text{mm}$, which consists of a section of length $L_{m2} = 6.5\,\text{mm}$ (with continuous tapered width from 1.9 mm to 0.77 mm) and another section with constant width 0.77 mm and length $L_{m1} = 3.25\,\text{mm}$ (corresponding to $\lambda/4$ based on the smallest frequency), was used as a feeding element at both ends. The tapering was made in order to improve matching characteristics at the input and output ports of the antenna. Instead of the usual triangular tapering, an exponential tapering was used. The tapered width $W_T = 1.9\,\text{mm}$ is decreasing exponentially over a distance equal to L_{m2}.

2.2. Antenna Design

There are two types of waves that an LWA can support: the slow wave, which has a phase velocity smaller than the speed of light in free space, and the fast wave, which has a phase velocity larger than the speed of light in free space. In order to radiate, an LWA should operate in the fast-wave region. By etching a series of slots on the top copper plane of the dielectric layer, a periodicity is introduced and the wave leaks out energy through the slots. In the case of a quasi-uniform LWA, the period, i.e., the distance between two adjacent slots, is very small compared to the wavelength, and radiation occurs from the fundamental space harmonic ($n = 0$). The fast-wave region is satisfied by the following equation [1]:

$$0 < \beta < k_o \tag{1}$$

where β is the phase constant, and k_o is the wavenumber of an unbounded wave in free space. In LWAs, the main radiation beam points in different directions as the frequency changes. The angular orientation of the main beam is given by [2]

$$\sin\theta_o = \frac{\beta}{k_o} \tag{2}$$

where θ_o is measured from broadside. Substituting Eq. (1) into Eq. (2), it is observed that the main beam of a quasi-uniform LWA can scan only in the forward quadrant. Its beamwidth is given by [2]

$$\Delta\theta = \frac{\lambda_o}{L_r \sin\theta_o} \tag{3}$$

where L_r is the radiating length of the antenna. Usually, the antenna should be sufficiently long so that approximately 90% of the propagating wave energy leaks out before the wave reaches the end of the guide. In SIW structures, in order to prevent significant leakage through vias, the following condition should be satisfied [24]:

$$\frac{s}{d} < 2.5 \tag{4}$$

The corresponding cut-off frequency of the SIW is calculated based on its equivalent rectangular waveguide. For the TE_{10} mode, it is given by [25]

$$f_c = \frac{c}{2W_{\mathit{eff}}\sqrt{\epsilon_r}} \tag{5}$$

where c is the speed of light in vacuum. The width W of the SIW and its equivalent rectangular-waveguide width, W_{eff}, are inter-related by the following expression [26]

$$W_{\mathit{eff}} = W - 1.08\left(\frac{d^2}{s}\right) + 0.1\left(\frac{d^2}{W}\right) \tag{6}$$

which is accurate for $s/d < 3$ and $d/W < 0.2$.

2.3. Liquid Crystal Properties

Liquid crystals are states of matter whose properties are somewhere between those of conventional liquids and those of solid crystals. More precisely, they behave like conventional crystalline solids below a critical temperature, T_m, and like isotropic liquids above a threshold upper temperature, T_c [27, 28]. They exist in different states but the most commonly-used form is the nematic state in which the molecules are rod-like and sensitive to an externally bias electric or magnetic field.

The most important feature of liquid crystals is their tuning capability that is based on the deflection characteristic of their optical axis. This optical axis coincides with the director of LC molecules [27]. If a bias voltage is applied across an LC cell, an electrostatic field is created within the crystal causing the orientation of the LC molecules to change according to the strength of the bias field [11]. This results to a change in the effective complex permittivity of the compound because the dielectric properties of liquid crystals are dependent on the relative angle between the directors and the orientation of the bias field. As a result, the propagation characteristics of the microwave or millimeter-wave device change accordingly [27].

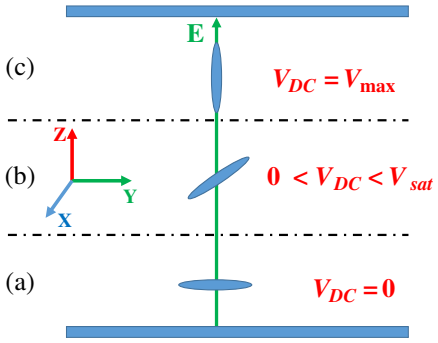

Figure 2. Biasing an LC cell using an externally applied DC voltage.

The operating principle of an LC cell under a bias voltage is illustrated pictorially in Fig. 2. As illustrated, when $V_{DC} = 0\,\text{V}$ (unbiased state), the directors of the LC cell are oriented in parallel to the surface layer (Fig. 2(a)). In this case, the permittivity of the LC compound corresponds to $\epsilon_\perp$ as the directors are oriented perpendicular to the direction of the bias electric field. Based on the right-handed coordinate system depicted in Fig. 2, the LC directors are oriented in the y-direction, and therefore, the homogeneous permittivity tensor for a uniaxial nematic LC is given by [27]:

$$\bar{\bar{\epsilon}}_\perp = \bar{\bar{\epsilon}}(V_{DC} = 0) = \begin{bmatrix} \epsilon_\perp & 0 & 0 \\ 0 & \epsilon_\parallel & 0 \\ 0 & 0 & \epsilon_\perp \end{bmatrix} \tag{7}$$

For the biased state ($V_{DC} = V_{\max} > V_{sat}$), the permittivity of the LC compound corresponds to $\epsilon_\parallel$. The LC directors point in the z-direction (see Fig. 2(c)) and the corresponding permittivity tensor is given by [27]:

$$\bar{\bar{\epsilon}}_\parallel = \bar{\bar{\epsilon}}(V_{DC} = V_{\max}) = \begin{bmatrix} \epsilon_\perp & 0 & 0 \\ 0 & \epsilon_\perp & 0 \\ 0 & 0 & \epsilon_\parallel \end{bmatrix} \tag{8}$$

For a biased state where $0 < V_{DC} < V_{sat}$, the director orientation forms an acute angle with respect to the z-direction, and as a result, the entries of the equivalent permittivity tensor of the LC take intermediate values. Calculation of the tensor entries for any bias voltage require the solution of a partial differential equation (PDE) obtained from the minimization of the Oseen-Frank functional. The particular non-linear PDE can be solved using the finite difference or the finite element methods. This approach is illustrated in [19] for the case of a frequency-agile patch antenna on top of a biased LC cell.

The difference between the permittivities of the two biasing states of LC is called dielectric anisotropy, and it is defined as:

$$\Delta\epsilon = \epsilon_\parallel - \epsilon_\perp \tag{9}$$

For a significant tuning ability, it is highly important that the dielectric anisotropy is as large as possible. New generation of nematic LCs are characterized by large dielectric anisotropy and very low loss tangent, deeming this type of substrates suitable for antenna design and fabrication.

3. SIMULATED RESULTS

In this section, we examine two specific LWA designs: a) one without the LC cell, and b) one with a thin layer of nematic LC underneath the Rogers substrate. For the latter, the simulations are carried out for the unbiased and fully biased case. The optimization of the two designs and the electromagnetic simulations presented in this paper were done using the High Frequency Structure Simulator (HFSS version 19).

3.1. LWA Design without Liquid Crystal

The geometry of the finalized SIW-LWA design without an LC cell was presented in Section 2.1. This particular antenna was designed to operate between 24.25 GHz and 29 GHz. Fig. 3 depicts the magnitudes of the S_{11} and S_{21} of the proposed antenna in the frequency band of interest. As illustrated, the S_{11} parameter is approximately below -10 dB in the entire frequency band and lower than -15 dB from 25.9 GHz to 29 GHz. This indicates good impedance matching at the input port of the antenna, which was achieved using exponential tapering of the feeding microstrip line; the vias and the rectangular slots were tapered linearly. At lower frequencies, the S_{21} parameter is relatively high due to the very small attenuation constant of the leaky-wave mode. When the frequency increases (from 24.25 GHz to 27.8 GHz), S_{21} slightly decreases since the attenuation of the leaky-wave mode increases. From 27.8 GHz and higher, S_{21} sharply increases, and the antenna enters the end-fire radiation region.

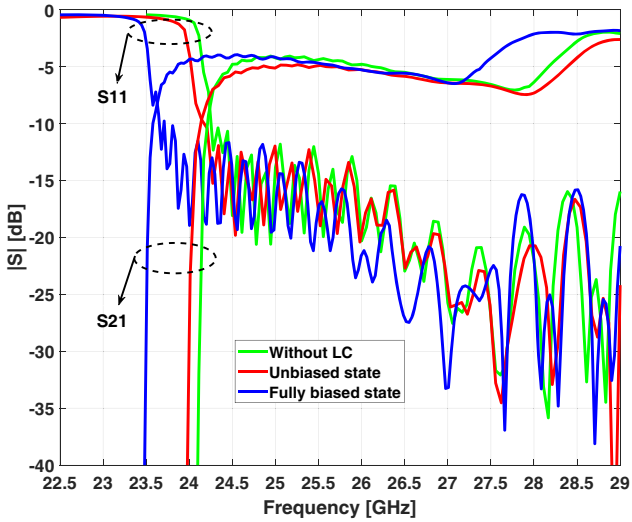

Figure 3. S-parameters of the proposed LWA with and without liquid crystal for biased and unbiased states.

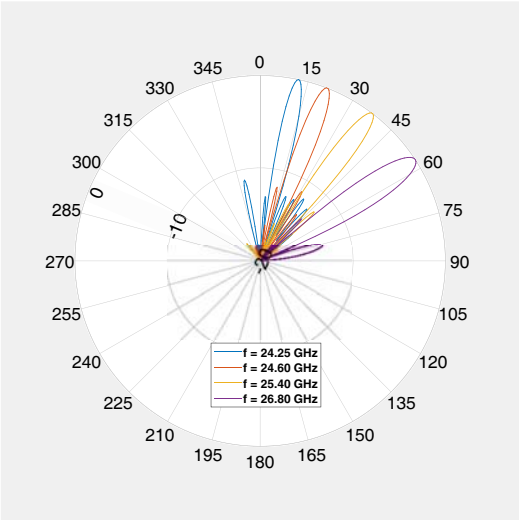

Figure 4. Normalized radiation pattern in the yz plane ($\phi = 90$) at different frequencies: 24.25 GHz, 24.60 GHz, 25.40 GHz and 26.80 GHz.

Figure 4 shows the normalized radiation pattern of the aforementioned LWA at different frequencies. As it is observed, the main beam scans from near broadside to end-fire in the forward quadrant; i.e, from 14° to 58° as the frequency increases from 24.25 to 26.80 GHz. The corresponding beamwidth also increases as frequency becomes higher. Figs. 5 and 6 illustrate the same type of radiation pattern but at 27.5 and 28 GHz, respectively. As shown, when the main radiation beam approaches the end-fire direction, the beamwidth becomes wider.

3.2. LWA Design with Liquid Crystal

In order to utilize the tunability of the LC for the design of a beam-steerable LWA at a single frequency, a very thin layer of LC cell has been placed between the substrate layer and the ground plane. In order

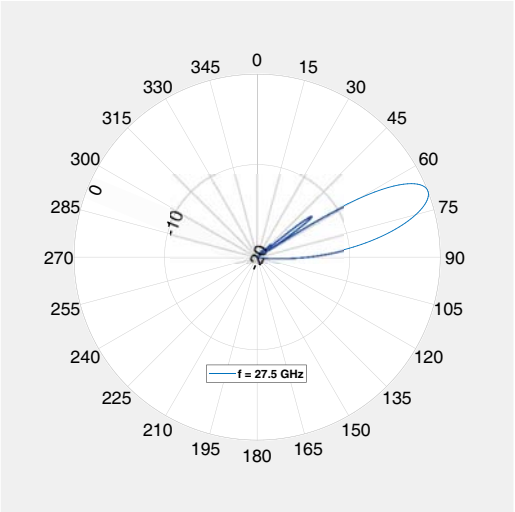

Figure 5. Normalized radiation pattern in the yz plane ($\phi = 90$) at 27.5 GHz.

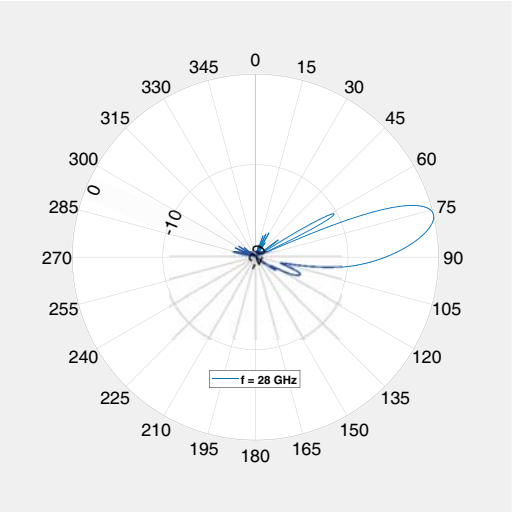

Figure 6. Normalized radiation pattern in the yz plane ($\phi = 90$) at 28 GHz.

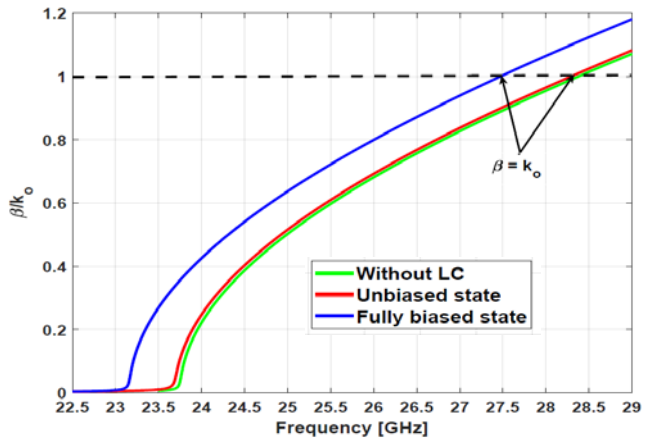

Figure 7. Dispersion curve of the proposed SIW structure.

to avoid shorting the upper and lower ground planes with the conducting vias, a thin annular slot could be etched around each via, thus creating electrical isolation. A DC voltage is then imposed between the upper and lower ground planes thereby creating a vertical electric field inside the nematic LC compound. It is worth emphasizing at this point that this is a concept LWA design aiming at demonstrating using numerical simulations the effect of liquid-crystal biasing on the direction of the main radiation beam. Due to the extreme difficulty of fabricating LWA in the mm-wave range, especially when the antenna incorporates liquid compounds that must be carefully sealed to avoid leakage, this particular design will be tested and evaluated numerically only.

The LC layer has a thickness of 50 µm and a width equal to the width of the substrate. The type is GT5-28004 and its perpendicular and parallel dielectric constants are 2.4 and 3.32 resulting in a dielectric anisotropy equal to 0.92. The material loss tangents are 0.0043 and 0.0014 for perpendicular and parallel orientations, respectively. The corresponding dispersion curve of the SIW structure is shown in Fig. 7 for two biasing conditions of the LC cell. According to this β-curve, the antenna can produce a single beam in the forward region of interest because the β-curve is located in the radiation region below the air line. In addition, by changing the bias voltage, the governing phase constant (β) at a given frequency changes accordingly. The range of possible values reside between the two curves which correspond to the fully biased and unbiased states. As shown in the figure, the corresponding phase constant of the LWA without LC is almost identical to that with LC in the unbiased state. It is quite obvious that the strength of the bias voltage — usually between 0 and 5 Volts — can significantly affect

the value of the propagation constant at a fixed frequency. Based on Eq. (2), it can be deduced that by changing the phase constant of the propagation mode, the main radiation beam can be dynamically scanned in the upper space. From Fig. 7, it can also be observed that the two phase constants (biased and unbiased states) converge to each other as the frequency increases. Hence, the range of scanning angles is expected to decrease with the increase in frequency.

A comparison of the antenna scattering parameters with and without liquid crystal is presented in Fig. 3. For the LC-based antenna, the corresponding S-parameters are shown for the fully biased and unbiased states. It is clearly shown that the antenna cut-off frequency for the unbiased state has been shifted toward lower frequencies by 125 MHz compared to the cutoff frequency of the antenna without LC. For the fully biased state, this frequency shift becomes 625 MHz, which is attributed to the dielectric anisotropy of the LC compound. The dielectric anisotropy of the LC used is $\Delta\epsilon = \epsilon_{\parallel} - \epsilon_{\perp} = 3.32 - 2.4 = 0.92$. The discrepancy between $\epsilon_{\perp} = 2.4$ and the dielectric constant of the substrate (2.33) is very small, and that is why a very small frequency shift is observed between the unbiased state and the antenna without liquid crystal.

Including liquid crystals in the antenna design affects impedance matching at the input port; thus, a new microstrip line width was calculated based on the total thickness of substrate and LC layer. This is due to the fact that the input impedance depends on substrate permittivity and thickness. The permittivity of the LC layer, which depends on the external bias voltage, alters the overall effective permittivity of the structure, thus affecting input impedance and matching at the input port. In our design, the S_{11} parameters, for the biased and unbiased states, are lower than -10 dB for all frequencies of interest. To obtain the new S-parameters with the LC layer in place, a new microstrip line width has been calculated based on the average permittivity of the LC (for the fully biased and unbiased states) and the substrate. It is worth emphasizing here that the cut-off frequencies in the S-parameters graph are slightly shifted compared to those shown in the dispersion diagram. This is attributed to the presence of the radiating slots on the top copper plate which tend to perturb the governing fields and surface currents of the propagating mode.

The normalized radiation patterns of the antenna for the two bias states (fully biased and unbiased) are shown in Fig. 8. The thickness of the LC is 50 µm and the corresponding operating frequencies are 24.5 GHz and 26 GHz (left to right). The scanning range decreases from 14° to 12°, respectively, as the operating frequency increases from 24.5 GHz to 26 GHz. This result is in good correlation with the dispersion curve shown in Fig. 7. As pointed out, the dispersion curves for the two states (fully biased and unbiased) tend to converge to each other as the frequency increases, thus resulting in lower scanning range. However, if the frequency approaches the point where the phase constant is equal to the wavenumber for free space (e.g., 27.5 GHz), the corresponding scanning range drops to 2° and radiation is end-fire.

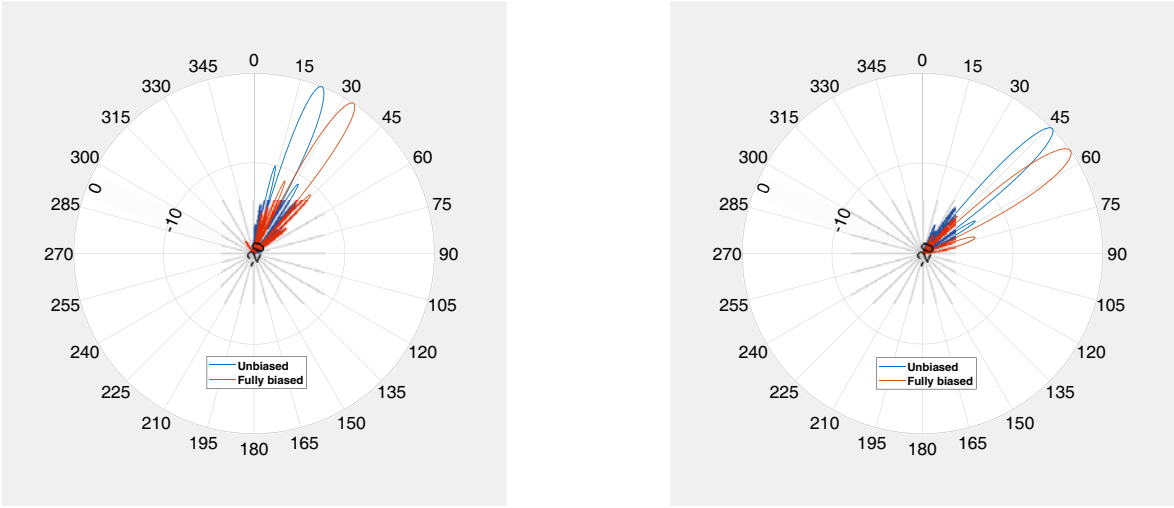

Figure 8. Normalized radiation patterns for the LC-based antenna at 24.5 GHz and 26 GHz (left and right, respectively); yz plane ($\phi = 0$).

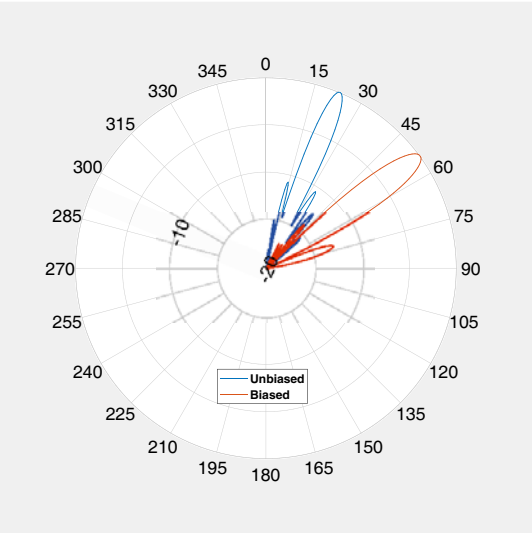

Figure 9. Normalized radiation pattern (yz plane) at 24.5 GHz for a thicker LC layer (100 µm) and a thinner substrate (127 µm).

Increasing the thickness of the liquid crystal layer or decreasing the substrate thickness results in a wider scanning range, as depicted in Fig. 9. In this particular case, where the thickness of the LC is doubled and the substrate thickness is reduced by half, the angular scanning range of the antenna at 24.5 GHz becomes 30° (as compared to 14°), which is more than double the previous value. Moreover, it is worth noting that the angular scanning range also depends on the LC dielectric anisotropy; i.e., $\Delta\epsilon$. The bigger the $\Delta\epsilon$ is, the wider the angular scanning range will be. To illustrate this dependence, a number of simulations were performed with different types of LC cells having thickness of 50 µm and a substrate thickness of 254 µm. Table 1 tabulates the type of LC compound used along with the respective dielectric anisotropy and the resulting scanning range at 24.5 GHz. As shown, the angular scanning range of the antenna at a fixed frequency can be significantly improved if a liquid crystal compound with large dielectric anisotropy is judiciously chosen for the particular antenna design.

Table 1. Scanning range at $f = 24.5$ GHz for different types of LCs.

LC types	$\Delta\epsilon$	$\Delta\theta$
E7	0.48	7°
GT3-23001	0.82	10°
GT5-28004	0.92	14°
Merck-MHT	1.08	16°
Merck-MixB	1.32	17°

4. CONCLUSION

In this paper, the fundamental properties of liquid crystal are applied in a quasi-periodic SIW leaky-wave antenna. The antenna was simulated using HFSS v.19 in order to illustrate that the main radiation beam can be dynamically scanned over a range of angles using a thin, biased liquid-crystal cell underneath the substrate. The return loss, gain, directivity, and scanning ability were optimized in order to satisfy performance criteria for a small-cell antenna operating at a future 5G frequency band. The paper illustrates only simulation results of this concept design as to the immense challenge to fabricate a high-frequency antenna with geometrical details and difficult-to-handle liquid compounds. As illustrated, the antenna scans in the forward quadrant starting from near broadside to end-fire as the frequency increases. In addition, the proposed antenna design is able to scan at a single frequency using a biased

LC cell. The scanning range of the designed antenna falls between 12° and 14° in the frequency band of interest, but it can surely reach more than 30° if one increases the ratio of LC-cell thickness to substrate thickness by a factor of 2.

REFERENCES

1. Jackson, D. R. and A. A. Oliner, "Leaky-wave antennas," *Modern Antenna Handbook*, Chap. 7, C. A. Balanis, ed., Wiley, New Jersey, NJ, USA, 2008.
2. Oliner, A. A. and D. R. Jackson, "Leaky-wave antennas," *Antenna Engineering Handbook*, 4th Edition, Chap. 11, J. L. Volakis (ed.), McGraw-Hill, NY, USA, 2007.
3. Che, W., D. Wang, K. Deng, and Y. L. Chow, "Leakage and ohmic losses investigation in substrate-integrated waveguide," *Radio Science*, Vol. 42, No. 5, 1–8, Oct. 2007.
4. Xu, F., K. Wu, and X. Zhang, "Periodic leaky-wave antenna for millimeter wave applications based on substrate integrated waveguide," *IEEE Trans. Antennas Propag.*, Vol. 58, No. 2, 340–347, 2010.
5. Monticone, F. and A. Alu, "Leaky-wave theory, techniques, and applications: From microwaves to visible frequencies," *Proceedings of the IEEE*, Vol. 103, No. 5, 793–821, May 2015.
6. Liu, J., D. R. Jackson, and Y. Long, "Substrate integrated waveguide (SIW) leaky-wave antenna with transverse slots," *IEEE Trans. Antennas Propag.*, Vol. 60, No. 1, 20–29, Jan. 2012.
7. Oseen, C. W., "The theory of liquid crystals," *Trans. Faraday Soc.*, Vol. 29, 883–898, 1933.
8. Frank, F. C., "On the theory of liquid crystals," *Discussions of the Faraday Soc.*, Vol. 25, 19–28, 1958.
9. Kuki, T., H. Fujikake, H. Kamoda, and T. Nomoto, "Microwave variable delay line using a membrane impregnated with liquid crystal," *2002 IEEE MTT-S International Microwave Symposium Digest*, 363–366, Seattle, WA, USA, 2002.
10. Kuki, T., H. Fujikake, and T. Nomoto, "Microwave variable delay line using dual frequency switching-mode," *IEEE Trans. Microw. Theory Tech.*, Vol. 50, 2604–2609, Nov. 2002.
11. Dolphi, D., M. Labeyrie, P. Joffre, and J. P. Huignard, "Liquid crystal microwave phase shifter," *Electronic Lett.*, Vol. 29, No. 10, 926–928, May 1993.
12. Weil, C., S. Muller, P. Scheele, Y. Kryvoshapka, G. Lussem, P. Best, and R. Jakoby, "Ferroelectric- and liquid crystal-tunable microwave phase shifters," *3rd Europ. Micr. Conf.*, 1431–1434, 2003.
13. Guo, Z., Y. Liu, T. Yang, Lei, D. Jiang, B. Gan, and W. Cao, "Tunable substrate integrated waveguide bandpass filter using liquid crystal material," *2016 11th International Symposium on Antennas, Propagation and EM Theory (ISAPE)*, 763–765, 2016.
14. Ding, C., F. Meng, H. Mu, J. Qiao, C. Zhao, Q. Yuan, and Q. Wu, "Design of a filtering tunable liquid crystal phase shifter based on coplanar waveguide and split-ring resonators," *Liquid Crystals*, Vol. 46, No. 15, 2127–2133, May 2019.
15. Martin, N., P. Laurent, C. Person, P. Gelin, and F. Hubert, "Patch antenna adjustable in frequency using liquid crystal," *IEEE 33rd Eur. Microw. Conf.*, 699–702, Munich, Germany, 2003.
16. Bose, R. and A. Sinha, "Tunable patch antenna using liquid crystal substrate," *2008 IEEE Radar Conference*, 1–6, Rome, Italy, 2008.
17. Shetta, A. and S. F. Mahmouh, "A widely tunable compact patch antenna," *IEEE Antennas Wireless Propag. Lett.*, Vol. 7, 40–42, 2008.
18. Missaoui, S. and M. Kaddour, "Tunable microstrip patch antenna based on liquid crystals," *2016 XXIst International Seminar/Workshop on Direct and Inverse Problems of Electromagnetic and Acoustic Wave Theory (DIPED)*, 88–91, Tbilisi, 2016.
19. Polycarpou, A. C., M. A. Christou, and C. N. Papanicolaou, "Tunable patch antenna printed on a biased nematic liquid crystal cell," *IEEE Trans. Antennas Propag.*, Vol. 62, No. 10, 4980–4987, Oct. 2014.
20. Prasetiadi, A. E., O. H. Karabey, et al., "Continuously tunable substrate integrated waveguide band pass filter in liquid crystal technology with magnetic biasing," *Electronic Lett.*, Vol. 51, No. 20, 1584–1585, 2015.

21. Li, X., D. Jiang, and H. Yu, "Electrical biasing substrate integrated waveguide tunable band pass filter with liquid crystal technology," *Optik*, Vol. 14, 718–723, 2017.
22. Fu, Z., D. Jiong, and Y. Liu, "Miniaturized pattern reconfigurable HMSIW leaky-wave antenna based on liquid crystal tuning technology in millimeter wave band," *2019 IEEE MTT-S International Wireless Symposium (IWS)*, 1–3, Guangzhou, China, 2019.
23. Tchema, R. B. and A. C. Polycarpou, "Quasi-periodic leaky-wave antenna based on substrate integrated waveguide and liquid crystal technologies," *14th European Conference on Antennas and Propagation (EuCAP)*, 1–5, Copenhagen, Denmark, 2020.
24. Bozzi, M., M. Pasian, L. Perregrini, and K. Wu, "On the losses in substrate integrated waveguides," *37th Eur. Microw. Conf.*, 384–387, 2007.
25. Cassivi, Y., L. Perregrini, P. Arcioni, M. Bressan, K. Wu, and G. Conciauro, "Dispersion characteristic of substrate integrated rectangular waveguide," *IEEE Microwave and Wireless Components Letters*, Vol. 12, No. 9, 333–335, Sept. 2002.
26. Deslandes, W. and K. Wu, "Substrate integrated waveguide leaky-wave antenna: Concept and design considerations," *Proc. Asia-Pacific Microwave Conf. (APMC)*, Suzhou, China, 2005.
27. Collings, P. J. and M. Hird, *Introduction to Liquid Crystals: Chemistry and Physics*, 1st Edition, Taylor and Francis, CRC Press, London, 1997.
28. Khoo, I., *Liquid Crystals*, 2nd Edition, Wiley, Hoboken, NJ, USA, 2007.